International Journal of Control, Automation, and Systems (2015) 13(2):434-442 ISSN:1598-6446 eISSN:2005-4092
DOI 10.1007/s12555-014-0039-y http://www.springer.com/12555

Motion Control of a 6WD/6WS Wheeled Platform with In-wheel Motors to Improve Its Maneuverability

Changjun Kim, Ali Mian Ashfaq, Sangho Kim, Sunghoon Back, Youngsoo Kim, Soonwoong Hwang, Jaeho Jang, and Changsoo Han*

Abstract: Multi-axle driving mobile platform that are favored in special environments require high driving performance, steering performance, and stability. Among these, six wheel drive and six wheel steering vehicles hereinafter called 6WD/6WS, gain structural safety by distributing the load and reducing the pitching motion during rapid acceleration and braking. 6WD/6WS mobile platforms are favorable for military use, particularly in off-road operations because of their high maneuverability and mobility on extreme terrains and obstacles. 6WD vehicles that use in-wheel motors can generate independent wheel torque without a need for additional hardware. Conventional vehicles, however, cannot generate an opposite driving force on wheels on both sides. In an independent steering and driving system six-wheel vehicles show better performance than conventional vehicles. This paper discusses the improvement of the cornering performance and maneuverability of 6WD/6WS mobile platform using independent wheel torque and independent steering on each wheel. 6WD/6WS vehicles fundamentally have satisfactory maneuverability under low speed, and sufficient stability at high speed. Consequently, there should be a control strategy for improving their cornering performance using the optimum tire forces that satisfy the driver's command and minimize energy consumption. From the driver's commands (i.e., the steering angle and accelerator/brake pedal stroke), the desired yaw moment with virtual steering, desired lateral force, and desired longitudinal force are obtained. These three values are distributed to each wheel as torque and steering angle, based on the optimum tire force distribution method. The optimum tire force distribution method finds the longitudinal/lateral tire forces of each wheel that minimize cost function, which is the sum of the normalized tire forces. This paper describes a 6WS/6WD vehicle with improved cornering performance and the results are validated through TruckSim simulations.

Keywords: 6WD/6WS, independent steering, cornering performance, energy minimization, independent driving, optimum tire force distribution method, trucksim, virtual steering.

NOMENCLATURE

δ_w	Virtual Steering Angle
δ	Steering Wheel Angle
δ_i	Tire Wheel Angle of Each Wheel (i=1~6)
$\omega_\delta(V)$	Steering Angle Gain according to Vehicle Velocity
n	Gear ratio
T_i	Driving Shaft Torque of Each Wheel (i=1~6)
F_{xi}, F_{yi}	Longitudinal and Lateral Force of Each Wheel (i=1~6)
F_{zi}	Vertical Force of Each Wheel (i=1~6) from TruckSim
F_R, F_L	Longitudinal Force of Right and Left Side Wheels
F_{xdes}, F_{ydes}	Desired Longitudinal and Lateral Force
M_{zdes}	Desired Yaw Moment
$\gamma, \gamma_a, \gamma_{des}$	Yaw Rate, Actual Yaw Rate from TruckSim, and Desired Yaw Rate
$\beta, \beta_a, \beta_{des}$	Sideslip Angle, Actual Sideslip Angle from TruckSim, and Desired Sideslip Angle
V_x, V_a	Longitudinal Vehicle Velocity, Actual Vehicle Velocity from TruckSim
C_{af}, C_{am}, C_{ar}	Cornering Stiffness at Front, Middle, and Rear Wheels
l_f	Distance from Center of Gravity to Front Axle

Manuscript received January 15, 2014; revised June 19, 2014; accepted August 22, 2014. Recommended by Associate Editor Gon-Woo Kim under the direction of Editor Hyouk Ryeol Choi.

This work was supported by the research fund of Hanyang University (HY-2011-P).

Changjun Kim is with the CIM and Robotics Lab, Hanyang University, Sa-3 dong, Ansan, Korea (e-mail: aphate@hanyang.ac.kr).

Sangho Kim is with the Department of Mechanical Engineering, Hanyang University, Sa-3 dong, Ansan, Korea (e-mail: shkim83@hanyang.ac.kr).

Jaeho Jang is with the Robotics R&BD Group, Korea Institute of Industrial Technology, Sa-3 dong, Ansan, Korea (e-mail: jaeho @kitech.re.kr).

Ali Main Ashfaq, Sunghoon Back, Youngsoo Kim, and Soonwoong Hwang are with the Department of Mechatronics Engineering, Hanyang University, Sa-3 dong, Ansan, Korea (e-mails: ishfaqaries@gmail.com, airback@hyundai-rotem.co.kr, gwa600@gmail.com, hswfile@gmail.com).

Changsoo Han is with the Department of Robot Engineering, Hanyang University, Sa-3 dong, Ansan, Korea (e-mail: cshan@ hanyang.ac.kr).

* Corresponding author.

l_r	Distance from Center of Gravity to Rear Axle
K_v	Understeer Gradient
a_x, a_y	Longitudinal and Lateral Acceleration
m, m_s	Vehicle Mass and Sprung Mass
μ	Friction Coefficient
J	Cost Function
r	Tire Radius
R	Turning Radius
t	Tread
M_t, M_z	Moment by Lateral Forces, Moment by Longitudinal Forces
I_z	Yaw Moment of Inertia
h_s	Sprung Mass Height
g	Gravity

1. INTRODUCTION

Multi-axle mobile robots for special environments require high driving performance, steering performance, and stability. Among these robots, 6WD/6WS vehicles ensure structural safety by distributing the load and thus, reducing the pitch angle during rapid acceleration and braking. 6WD vehicles have better acceleration and braking forces than 2 wheel drive (2WD) or 4 wheel drive (4WD) vehicles, and they show excellent performance on rough or slippery roads and even in the case of failure of one or two wheels [1]. Using a mechanical steering system for a platform with more than two steering wheels would result in more complex structure and Ackerman geometry for such multi-axle platform will be difficult to achieve where all the wheels will have a common point to rotate about. [2]. this complexity can be solved using independent wheel steering system on all wheels.

For the independent wheel steering system, steer-by-wire is being actively studied for improved performance and enhanced safety. It allows independent control of left and right wheels by removing the steering column that connects the steering wheel to the steering mechanism. Because of the independent steering of front wheels by controller command, true Ackerman steering geometry can be achieved as well as active safety can be realized [3].

Vehicle stability control techniques, including active steering and yaw moment application, are being widely studied for 4WD vehicles [4]. M. Abe et al. applied the distribution of longitudinal/lateral tire force to 4WD vehicles to improve the vehicles stability [5]. The stability control technique for existing 4WD vehicles is being applied to 6WD vehicles. This seems a good means of improving the performance of 6WD platform that is equipped with in-wheel motor drive.

With the development of battery technology and in-wheel motors, multi-axle electric vehicles with in-wheel motors in each wheel, as well as general 4WD electric vehicles are being studied. These power drive systems have the following advantages in terms of control [8].

1) Very fast and accurate torque generation can be realized.
2) The torque created on the wheel can be easily estimated from motor current.
3) Motors can be mounted on individual wheels and can be controlled individually.

In general vehicles, the creation of a driving force difference between the left and right wheels requires a mechanical mechanism, e.g., the torque vectoring device (TVD). However, in vehicles with in-wheel motors, each wheel can be driven by the motor mounted on the wheel without the need for a mechanical device. Using independent drive and steering on each wheel, the turning radius can be reduced at low speed to improve maneuverability, and it can be raised at a high speed to improve stability.

This study is aimed to improve the maneuverability of 6WD/6WS mobile robot by distributing the steering and driving control inputs of the vehicle using the longitudinal/lateral tire force optimization method for 6WD/6WS vehicles and direct yaw moment control (DYC). The system considered in this study is a wheeled platform best suited for military application. Since many of the techniques discussed in the referred literature in introduction has been applied to conventional vehicle so the idea is to apply similar approach to improve the performance of 6 wheeled mobile robot at high speeds. For the analysis of this algorithm TruckSim software has been used. Wheeled mobile platform at high speed exhibit similar behavior to a conventional vehicle and hence the system can be studied from vehicle dynamics point of view. Eventually in the following sections of paper vehicle terminologies will appear for description and explanation.

This paper is organized as following. Section 2 introduces the 6WD/6WS platform dynamic model. Section 3 introduces the TruckSim vehicle model, to which the control algorithm in this study was applied. Section 4 proposes the control algorithm to improve the vehicle's cornering performance via comparing the desired model and the TruckSim model. Section 5 shows the simulation results and improvements of the applied vehicle. Finally, Section 6 presents the conclusion.

2. THE SIX-WHEELED MOBILE PLATFORM DYNAMIC MODEL

This paper uses a six-wheel platform model as shown in Fig. 1. The distances from the body center to the front and rear wheels are l_f and l_r, respectively. There was no distance from the body center to the middle wheels axis so $l_r = 0$.

The following motion equation represents the dynamics of the mobile robot motion at high speed.

$$mV_x\left(\dot{\beta}+\gamma\right)=\sum_{i=1}^{6}F_{yi}, \tag{1}$$

$$\begin{aligned} I_z\dot{\gamma} &= \left[\frac{t}{2}\left(F_{x2}+F_{x4}+F_{x6}-F_{x1}-F_{x3}-F_{x5}\right)\right] \\ &\quad +\left[l_f\left(F_{y1}+F_{y2}\right)-l_r\left(F_{y5}+F_{y6}\right)\right], \end{aligned} \tag{2}$$

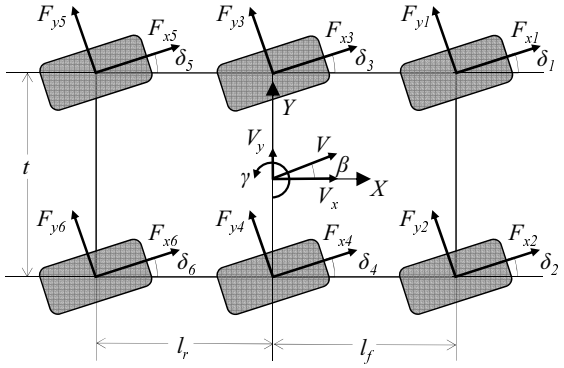

Fig. 1. Six-wheel mobile platform.

where

$$M_z = \frac{t}{2}\left(F_{x2} + F_{x4} + F_{x6} - F_{x1} - F_{x3} - F_{x5}\right),$$
$$M_t = l_f\left(F_{y1} + F_{y2}\right) - l_r\left(F_{y5} + F_{y6}\right),$$

where m is the vehicle mass, V_x is the longitudinal speed, β is the slip angle, I_z is the moment of inertia, γ is the yaw rate, t is the tread, which is the distance between the left and right wheels, and F_{xi} is the longitudinal force at the i[th] tire. The yaw moment consists of the direct yaw moment (M_z) due to the longitudinal driving force difference between the tires and the turning force moment (M_t) created from the tire during the turning as a resistive component.

2.1. Desired yaw moment

The steady-state steering angle for driving on roads with the turning radius R is given as

$$\delta = \frac{l_f + l_r}{R} + K_V a_y, \tag{3}$$

where K_V is the understeer gradient, which is given as follows:

$$K_V = \frac{l_r m}{2C_{\alpha f}\left(l_f + l_r\right)} - \frac{l_f m}{2C_{\alpha r}\left(l_f + l_r\right)}. \tag{4}$$

By substituting (4) into (3), the turning radius is expressed as follows:

$$\frac{1}{R} = \frac{\delta}{l_f + l_r + \dfrac{mV_x^{\,2}\left(l_r C_{\alpha r} - l_f C_{\alpha f}\right)}{2C_{\alpha r}C_{\alpha f}\left(l_f + l_r\right)}}. \tag{5}$$

The desired yaw rate is determined by the following equation according to the steering angle and the longitudinal speed. This will show some time delay for the steady state value of desired yaw rate and this is modeled as the first ordered system.

$$\frac{\gamma_{des}}{\delta} = k = \frac{V_x}{l_f + l_r + \dfrac{mV_x^{\,2}\left(l_r C_{\alpha r} - l_f C_{\alpha f}\right)}{2C_{\alpha r}C_{\alpha f}\left(l_f + l_r\right)}}, \tag{6}$$

$$\gamma_{des} = \frac{k}{1 + \tau_{system} s}\delta. \tag{7}$$

The desired yaw moment M_{zdes} is created using the PID controller to reduce the difference between the desired yaw rate given by (7) and the actual yaw rate of the model. Fig. 6 represents the signal generation of desired yaw moment.

2.2. Desired tire forces

The desired longitudinal acceleration (a_x^*) is created according to the driver's inputs. Therefore, the desired longitudinal force is defined as

$$F_{xdes} = ma_x^*. \tag{8}$$

As shown in Fig. 1, the sum of the longitudinal forces from the tires must be equal to the desired longitudinal force, which represents the driver's acceleration and braking intent.

$$\sum_{i=1}^{6} F_{xi} = F_{xdes} \tag{9}$$

From the steady-state yaw angle error, the steady-state slip angle is expressed as

$$\beta = \frac{l_r}{R} - \frac{l_f}{2C_{\alpha r}L}\frac{mV_x^{\,2}}{R}. \tag{10}$$

By substituting (5) into (10), the steady-state slip angle is calculated using the following equation.

$$\beta = \frac{l_r - \dfrac{l_f m V_x^{\,2}}{2C_{\alpha r}\left(l_f + l_r\right)}}{l_f + l_r + \dfrac{mV_x^{\,2}\left(l_r C_{\alpha r} - l_f C_{\alpha f}\right)}{2C_{\alpha r}C_{\alpha f}\left(l_f + l_r\right)}}\delta \tag{11}$$

After the slip angle is calculated, then the desired lateral force can be calculated from the derivative of the slip angle, yaw rate, and longitudinal speed.

$$F_{ydes} = mV_x\left(\dot{\beta} + \gamma\right), \tag{12}$$

$$\sum_{i=1}^{6} F_{yi} = F_{ydes}. \tag{13}$$

3. THE SIX WHEELED PLATFORM TRUCKSIM MODEL

In this study, the TruckSim model was chosen to address the multi-axle mobile platform. The propulsive transmission system was removed from the model in software to represent the in-wheel-motor architecture and the applied torques signals from the control algorithm were directly applied to the tires.

The data for the development of the TruckSim vehicle model included the mass, inertia, and dimension parameters of the sprung mass; the K&C data of the suspension system.

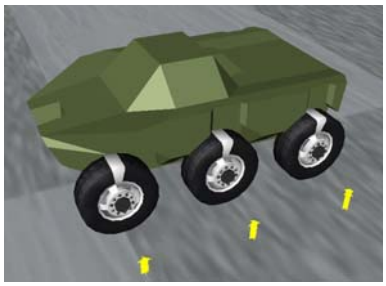

Fig. 2. Six wheeled mobile platform TruckSim model.

Table 1. Composition of the 6X6 TruckSim model.

	Parameters used in Simulation
Sprung mass	1.5 tons, wheelbase 2,320 mm, tread 1,830 mm
Suspension	Independent type Jounce stop: 106 mm, Rebound stop: 86 mm
Steering	Independent Steering from Algorithm
Tire	250 N/mm spring rate, 400mm radius
Brake	Mechanical brake

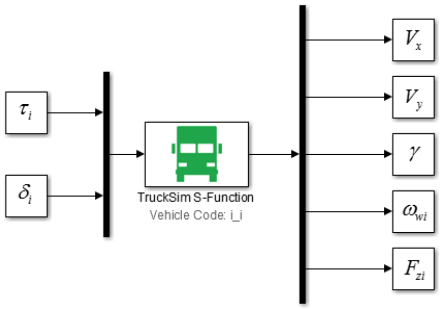

Fig. 3. The input and output of the TruckSim model.

Table 2. Input and output of the TruckSim vehicle model.

	Definition	Unit
τi	Drive shaft torque at each wheel (i = 1-6)	Nm
δ_i	Steering wheel input	deg
Vx	Longitudinal vehicle speed	kph
Vy	Lateral vehicle speed	kph
γ	Yaw rate	deg/s
ωwi	Speed of each wheel (i = 1-6)	rpm
Fzi	Vertical force of each wheel (i = 1-6)	N

Fig. 2 shows the 6X6 mobile platform TruckSim model. The weight, wheelbase and tread values used for the 6X6 model sprung mass are shown in Table 1. An independent suspension was used on all axles. TruckSim software is capable of dealing with nonlinearity associated with longitudinal/lateral motion of the tires and the caster/camber/toe changes. The steering angle at each wheel is calculated by the control algorithm as given in (21).

Fig. 3 and Table 2 show the inputs and outputs of the TruckSim model. Six torque values that generate driving force on the wheels were applied to the vehicle model. The outputs included the longitudinal/lateral speed, yaw rate, wheel speed, and vertical force.

Fig. 4 defines the torque performance curve using the maximum driving shaft torque. The RPM required for the pivot steering is shown using point A, and point B obtained during the 120kph constant speed driving. Point C is obtained by calculating the wheel torque and RPM

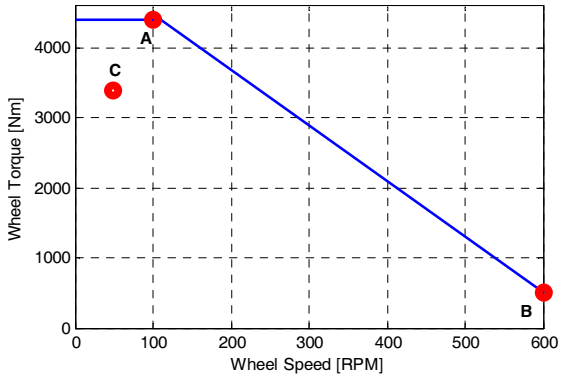

Fig. 4. Wheel torque and RPM performance curve of the electric in-wheel motor.

that are required for 60% slope climbing [7]. These points were obtained by carrying out several simulations of pivot steering maneuver, straight line motion at high speed and driving on steer slops. The torque performance curve is used as the basis for the choice of in-wheel motor torque at different speeds.

4. CONTROL ALGORITHM

The desired longitudinal force, desired lateral force and yaw moment are calculated from the driver's commands using two separate PID controllers as shown in Fig.6. Therefore, these desired values are used by the optimum tire force distribution algorithm to determine the longitudinal and lateral forces for each tire that can be realized by applied torques and steering angles on individual wheels.

4.1. Vertical tire loads

The tire vertical forces change with the longitudinal acceleration a_x and the lateral acceleration a_y, as shown in (14), which are readily available from the TruckSim model.

$$
\begin{aligned}
F_{z1} &= \frac{mgl_r}{3(l_f+l_r)} - \frac{m_s a_x h_s}{2l} - k_f \frac{m_s a_y h_s}{t}, \\
F_{z2} &= \frac{mgl_r}{3(l_f+l_r)} - \frac{m_s a_x h_s}{2l} + k_f \frac{m_s a_y h_s}{t}, \\
F_{z3} &= \frac{mg}{6} - k_m \frac{m_s a_y h_s}{t}, \\
F_{z4} &= \frac{mg}{6} + k_m \frac{m_s a_y h_s}{t}, \\
F_{z5} &= \frac{mgl_f}{3(l_f+l_r)} + \frac{m_s a_x h_s}{2l} - k_r \frac{m_s a_y h_s}{t}, \\
F_{z6} &= \frac{mgl_f}{3(l_f+l_r)} + \frac{m_s a_x h_s}{2l} + k_r \frac{m_s a_y h_s}{t},
\end{aligned}
\tag{14}
$$

where m_s is the sprung mass, h_s is the sprung mass height, g is the gravitational constant, and k_f, and k_r are the lateral weight-shift distributions on the front and rear wheels, respectively.

4.2. Optimized lateral and longitudinal tire force

In this study, the objective function was minimized using the Lagrange multiplier method for optimization, and the lateral and longitudinal forces to satisfy the desired longitudinal force F_{xdes}, desired lateral forces F_{ydes} and yaw moment M_{zdes} were calculated. The objective function is defined as the sum of the squared normalized forces on each tire from the concept of the friction circle [9]. This solution automatically guarantee the minimization of energy consumption for any given motion. This algorithm will cause the platform to move with little resistance during turning motion. Secondly the weight shifts during braking/acceleration or due to cornering motion are also taken into account, this will make sure that every wheel will be powered according to the vertical load it carries and the possibilities of slipping the wheels will be minimum. The objective function is given in

$$J = \sum_{i=1}^{6} \mu_i^2 = \sum_{i=1}^{6} \frac{F_{xi}^2 + F_{yi}^2}{F_{zi}^2}. \tag{15}$$

The constraint equations can be expressed as the following linear simultaneous equation:

$$\mathbf{Ax} = \mathbf{b}, \tag{16}$$

where

$$\mathbf{A} = \begin{bmatrix} 1 & 1 & 1 & 1 & 1 & 1 & 0 & 0 & 0 & 0 & 0 & 0 \\ 0 & 0 & 0 & 0 & 0 & 0 & 1 & 1 & 1 & 1 & 1 & 1 \\ -\frac{t}{2} & \frac{t}{2} & -\frac{t}{2} & \frac{t}{2} & -\frac{t}{2} & \frac{t}{2} & l_f & l_f & 0 & 0 & -l_r & -l_r \end{bmatrix},$$

$$\mathbf{x} = \begin{bmatrix} F_{x1} & F_{x2} & F_{x3} & F_{x4} & F_{x5} & F_{x6} & F_{y1} & F_{y2} & F_{y3} & F_{y4} & F_{y5} & F_{y6} \end{bmatrix}^{\mathrm{T}},$$

$$\mathbf{b} = \begin{bmatrix} F_{xdes} & F_{ydes} & M_{zdes} \end{bmatrix}^{\mathrm{T}},$$

F_{x1} to F_{x6} are responsible for the yaw moment M_z, while yaw moment M_t is obtained by F_{y1} to F_{y6}. The optimization issue can be redefined using the objective function in (15) and the constraint conditions in (16). Based on these the following problem is formulated.

$$\begin{aligned} &\text{minimize } \frac{1}{2} J = \frac{1}{2} \mathbf{x}^{\mathrm{T}} \mathbf{W} \mathbf{x} \\ &\text{subject to } \mathbf{b} - \mathbf{Ax} = 0, \end{aligned} \tag{17}$$

where

$$\mathbf{W} = \begin{bmatrix} F_{z1}^{-2} & & & & & \\ & \ddots & & & & \\ & & F_{z6}^{-2} & & & \\ & & & F_{z1}^{-2} & & \\ & & & & \ddots & \\ & & & & & F_{z6}^{-2} \end{bmatrix}.$$

The Lagrangian function for the optimization given in (17) is defined as follows:

$$L(\mathbf{x}, \boldsymbol{\lambda}) = \frac{1}{2} \mathbf{x}^{\mathrm{T}} \mathbf{W} \mathbf{x} + \boldsymbol{\lambda}^{\mathrm{T}} (\mathbf{b} - \mathbf{Ax}), \tag{18}$$

where $\boldsymbol{\lambda}$ is the Lagrangian multiplier. The gradient of the Lagrangian function in (18) must be zero when x minimizes the objective function, and

$$\mathbf{x} = \mathbf{W}^{-1} \mathbf{A}^{\mathrm{T}} \left(\mathbf{A} \mathbf{W}^{-1} \mathbf{A}^{\mathrm{T}} \right)^{-1} \mathbf{b}. \tag{19}$$

The solution of vector $\mathbf{x}$ have the values of lateral and longitudinal tire forces that minimizes the objective function in (15).

4.3. Driving torque and steering angles at each wheel

To realize independent driving of 6WD/6WS electric vehicles, a method was used to determine each wheel driving torque to generate the force on each tire.

When the tire radius is r, the driving torque of the i^{th} wheel is calculated from the following equation using the longitudinal tire force determined in (19).

$$T_i = r F_{xi} \tag{20}$$

The optimum driving torque for six-wheel mobile platform is determined based on the optimum tire force distribution method and the steering angle at each wheel is determined independently by the following equation

$$\delta_i = \begin{cases} \dfrac{F_{yi}}{C_{\alpha f}} + \beta + \dfrac{l_f \gamma}{V_x} & \text{for } i = 1,2 \\ \dfrac{F_{yi}}{C_{\alpha m}} + \beta & \text{for } i = 3,4 \\ \dfrac{F_{yi}}{C_{\alpha r}} + \beta - \dfrac{l_r \gamma}{V_x} & \text{for } i = 5,6. \end{cases} \tag{21}$$

4.4. Virtual steering angle algorithm

The virtual angle algorithm minimizes the turning radius to improve vehicle maneuverability at a low speed and stability at a high speed. This has the same concept as variable gear ratio, which increases the front wheel steering angle at a low speed to the driver steering wheel input, and decreases the steering input at a high speed.

The steering angle of tire δ_w is calculated from the driver's steering input δ, as in (21), with n as the steering gear ratio:

$$\delta_{\mathrm{w}} = \frac{\omega_\delta(V)}{n} \delta, \tag{22}$$

where ω_δ is the steering angle gain determined by the vehicle speed, as shown in Fig. 5. The value was determined via a simulation according to the vehicle performance that resulted in stable motion at different speeds.

4.5. Equivalent tire force distribution

For comparison with the tire optimum driving force distribution method, the equivalent tire force distribution method can be expressed as follows:

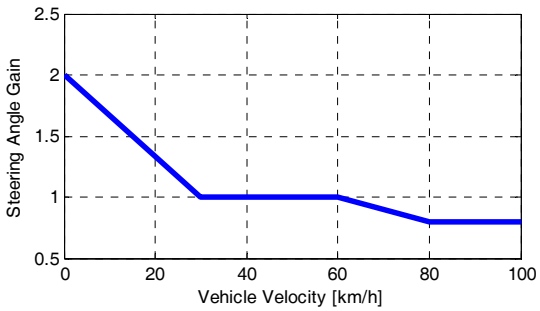

Fig. 5. Virtual steering angle gain (ω_δ) according to the vehicle velocity.

$$F_R = \frac{(t/2)F_{\text{xdes}} + M_{\text{des}}}{l_t}, \tag{23}$$

$$F_L = \frac{(t/2)F_{\text{xdes}} - M_{\text{des}}}{l_t}, \tag{24}$$

whereas F_R and F_L are the longitudinal forces of the right and left wheels, respectively and t is the tread, which is the distance between the left and right wheels. This method represents the mobile platform where all the wheels on same sides are connected via chain or belts and are constraint to rotate with same speeds [2].

5. SIMULATION AND VERIFICATION

Fig. 6 shows the block diagram of the six-wheel vehicle control algorithm based on the optimum tire force distribution method. The desired speed is compared with the platform speed to calculate the desired longitudinal force F_{xdes} using a PID controller. This represents the total driving force required to the move the platform with the desired velocity in a close loop control.

Using the driver's commands of acceleration and steering wheel angle the desired yaw rate is calculated, which is then used to calculate the desired yaw moment. Based on the yaw moment, longitudinal force, and vertical tire force, the driving torque is determined from the optimum tire force distribution block diagram. The results of the optimum tire force distribution were the longitudinal and lateral tire forces, and the longitudinal tire forces were converted into the driving torque using (18) and lateral tire forces are used to calculate the steering angles at each wheels using (21).

5.1. Minimization of the turning radius at low speed

Fig. 7 shows the simulation results of the turning radius minimization at a low speed using the virtual steering angle algorithm. It shows the vehicle trajectories comparison with and without this algorithm. A 25kph vehicle speed and a maximum steering wheel angle of 10° of driver input were applied to the simulation when the virtual steering angle algorithm. As can be seen from the figure the virtual steering angle minimized the turning radius as desired at low speed. This was because of the increased desired yaw rate according to the virtual steering angle, and the direct yaw moment control (DYC).

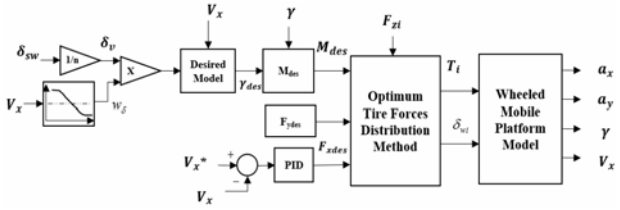

Fig. 6. Block diagram of the six-wheel vehicle control algorithm.

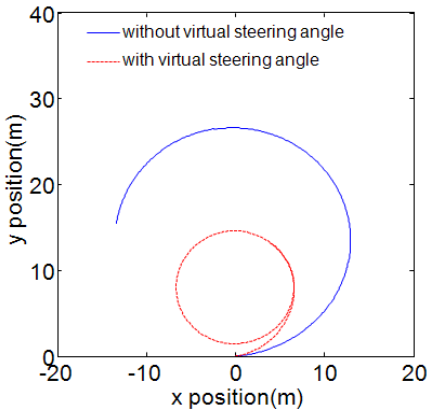

Fig. 7. Vehicle turning radius at a low speed.

5.2. Improvement of the vehicle stability at a high speed

The turning stability is important at a high speed maneuvers. In the virtual steering angle algorithm, the desired yaw rate can be reduced by decreasing the steering angle of the wheel to improve the turning stability. This was comparatively simulated as follows. At a vehicle speed of 60 kph, a 3° wheel steering angle was applied, and the results before and after the application of the virtual steering angle algorithm were comparatively analyzed. The results showed that the yaw rate decreased when the virtual steering angle algorithm was used, as shown in Fig. 8, and the vehicle with the virtual steering angle had a greater understeer tendency than that without a virtual steering angle.

5.3. Optimum tire force distribution algorithm simulation

To verify the effect of the optimum tire force distribu-

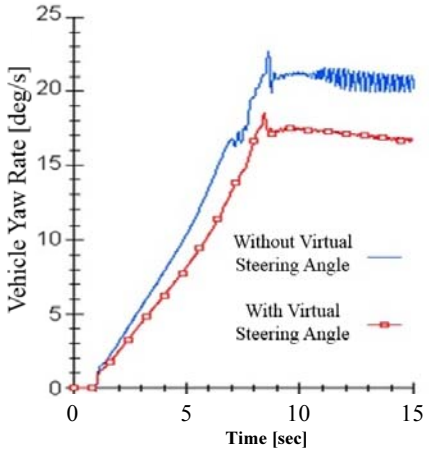

Fig. 8. Comparison of the yaw rate at a high velocity.

tion algorithm, which minimizes the sum of the tire work loads, the optimum distribution algorithm was compared with the equivalent tire force distribution algorithm. The vehicle was accelerated and decelerated during turning, and the driving forces of the tires due to the turning operation were considered.

Fig. 10 shows the performance index J when the optimum tire force distribution algorithm and the equivalent tire force distribution algorithm were applied to the aforementioned profile, as shown in Fig. 9. The results show that J is smaller in the optimum distribution algorithm. This indicates that the lateral force was reduced by the hybrid steering effect due to the optimum tire force distribution algorithm. The proposed vehicle control algorithm can be verified using the results of the performance index J. Fig. 11 shows the components of Performance Index. Each component converges to minimum value so that each tire is loaded with minimum power for energy minimization.

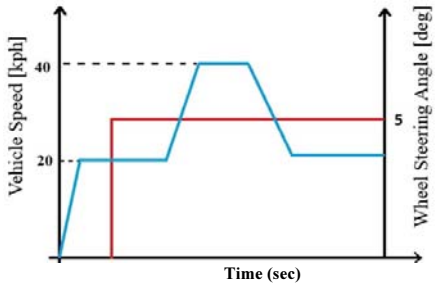

Fig. 9. Profile of the vehicle speed and the steering angle.

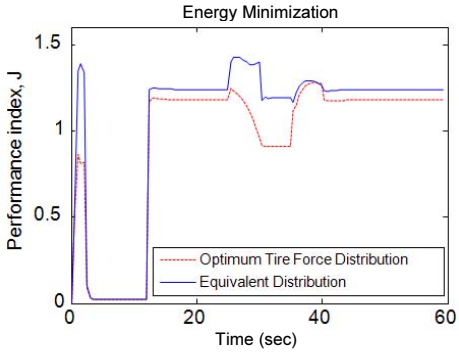

Fig. 10. Performance index j of the equivalent and optimum tire force distribution method.

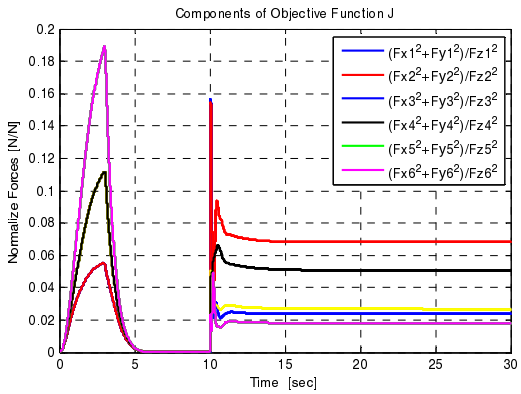

Fig. 11. Components of performance index J.

5.4. Turning radius and drivable lateral acceleration by vehicle speed

Figs. 12 and 13 show the turning radius and the drivable lateral acceleration by vehicle. Fig. 12 shows the results of the equivalent tire force distribution method.

Different lateral acceleration g lines are drawn on these plots. This Fig. shows that a steering angle of 135 degree when applied at 40 kph will produce a lateral acceleration of 0.7 g using equivalent tire force distribution method (ETFDM). Fig. 13 shows the optimum tire force distribution, which was used in this study. The turning radius was minimized at a low speed and increased at a high speed to ensure stability. The gain of VSA algorithm is tuned by carrying several simulations and the steering sensitivity is designed such that at any speed the motion of mobile platform will remain stable with minimum chance of rollover.

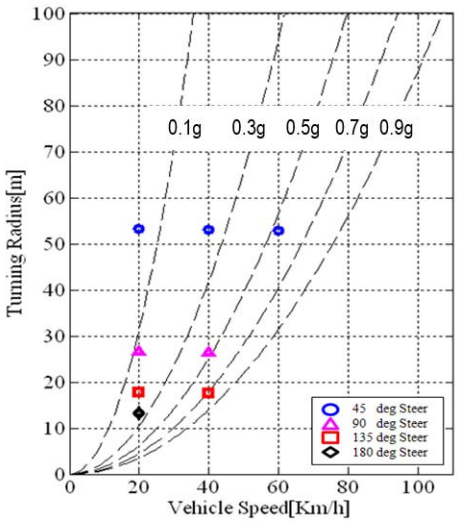

Fig. 12. Turning radius and lateral acceleration with respect to the vehicle velocity for the equivalent tire force method.

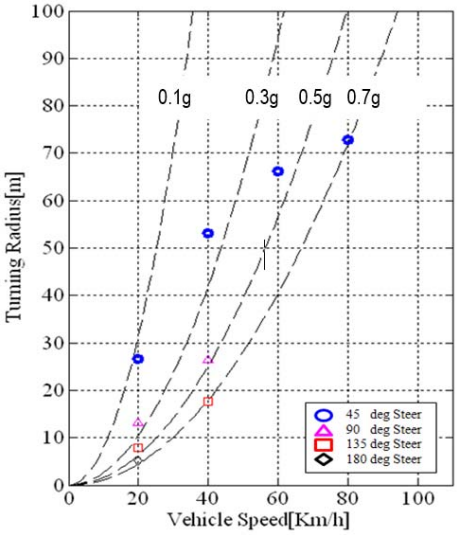

Fig. 13. Turning radius and lateral acceleration with respect to the vehicle velocity for the optimal tire force method.

The graph shows the turning radius and lateral acceleration when the vehicle speeds were 20, 40, 60, and 80 kph with steering angles of 45, 90, 135, and 190°. The results show that the cornering performance of the optimum tire force distribution vehicle improved.

6. CONCLUSION

In this study is focused on devising a control algorithm for a six-wheeled mobile platform which is equipped with in-wheel motors and have independent steering system on each wheel. Such a system have redundancy in realizing a maneuver and several types of control algorithms may be devised for this. The focus point in this study was the minimization of energy consumption while at the same time improving the maneuverability at low speed and ensuring the safety at high speed. The following are the results of the study of the control algorithm for improved cornering performance of six wheeled mobile robot platform.

1) The TruckSim model was used to verify the control algorithm.
2) The sprung mass, tire, suspension, brake, and steering of the TruckSim model were used as the model with the propulsive transmission system removed to represent the in-wheel-motor electric vehicle architecture. The detailed model exhibit the performance of real system and is capable of handling all the nonlinearity of actual system.
3) The turning radius was reduced at a low speed, and the virtual steering angle was used to improve the vehicle stability at a high speed for a stable motion without the danger of rollover by keeping the lateral acceleration within limit.
4) The yaw rate that was created by the virtual steering angle controlled the driving force of each wheel and produced the direct yaw moment control (DYC) effect to improve the maneuverability and stability of the 6WD vehicle.
5) The optimum tire force distribution method distributed the driving force to each wheel by minimizing the objective function. The objective function in this study is made of sum of square of lateral and longitudinal tire forces and minimizing such an objective function means that the mobile platform would achieve the desired motion with minimum torques and steering efforts.
6) To verify the energy minimization effect, J was examined in the equivalent distribution method and in the optimum distribution method. The results showed an energy minimization effect.
7) The results of the comparative analysis of the turning radius and drivable lateral acceleration by vehicle speed using the proposed algorithm showed that the cornering performance of the vehicle improved.

Further studies will need to address fail-safe conditions in the case of in-wheel motor faults, and estimate the vehicle status for the application of the algorithm to actual vehicles.

REFERENCES

[1] K.-S. Huh, K.-Y. Jhang, J.-E. Oh, J.-Y. Kim, and J.-H. Hong, "Development of a simulation tool for the cornering performance analysis of 6WD/6WS vehicles," *Journal of Mechanical Science and Technology*, vol. 13, no. 3, pp. 211-220, 1999.

[2] J. C. Fauroux, "Modeling, experimenting, and improving skid steering on a 6x6 all-terrain mobile platform," *Journal of Field Robotics*, vol. 27, no. 2, pp. 107-126, 2010.

[3] C.-J. Kim, J.-H. Jang, S.-N. Yu, S.-H. Lee, C.-S. Han, and J. K. Hedrick, " Development of a control algorithm for a tie-rod-actuating steer-by-wire system," *IMechE Part D, Journal of Automobile Engineering*, vol. 222, no. 9, pp. 1543-1557, 2008.

[4] M. Nagai, Y. Hirano, and S. Yamanaka, "Integrated control of active rear wheel steering and direct yaw moment control," *Vehicle System Dynamics*, vol. 27, no. 5-6, pp. 357-370, 1997.

[5] O. Mokhiamar and M. Abe, "Simultaneous optimal distribution of lateral and longitudinal tire forces for the model following control," *Journal of Dynamic Systems, Measurement, and Control*, vol. 126, no. 4, pp. 753-763, 2004.

[6] M.-A. Ali, C.-J. Kim, H.-S. Shin, J.-H. Jang, and C.-S. Han, "Study on the characteristics of skid steering for six wheel drive vehicle (6x6)," *Proc. of the Korean Society of Automotive Engineers Fall Conference*, p. 325, 2008.

[7] H. Fujimoto, T. Saito, A. Tsumasaka, and T. Noguchi, "Motion control and road condition estimation of electric vehicles with two In-wheel motors," *Proc. of IEEE Int. Conference on Control Applications*, pp. 1266-1271, 2004.

[8] Y. Hori, Y. Toyoda, and Y. Tsuruoka, "Traction control of electric vehicle: basic experimental results using the test EV, UOT," *IEEE Trans. Ind. Applicat.*, vol. 34, no. 5, pp. 1131-1138, 1998.

[9] R. Rajamani, *Vehicle Dynamics and Control*, Springer, 2012.

Changjun Kim received his B.S. degree in Mechanical Engineering from Hanyang University in 2004; an M.S. degree in Mechatronics Engineering from Hanyang University in 2006; and a Ph.D. degree in Mechanical Engineering from Hanyang University in 2012. He is currently doing Post Doctor at CIM and Robotics Lab. His research interests include robotic vehicle, electric vehicle with in-wheel motors, and vehicle dynamics (independent steering, active steering and driving, and hybrid driving).

Ali Mian Ashfaq received his B.S. degree in Mechanical Engineering from N.W.F.P University of Engineering and Technology Peshawar Pakistan, and his M.S. degree in Mechanical Engineering from Hanyang University in 2010. He is currently doing a Ph.D. degree in Mechatronics Engineering from Hanyang Uni-

versity. He is researching skid steering multi-axle vehicle, electric vehicle with in-wheel-motor drive, wheel dynamics and control.

Sangho Kim received his B.S. degree in Mechanical Engineering from Hanyang University in 2010. He is currently working toward a M.S. leading to Ph.D. degree in Mechanical Engineering at Hanyang University. His research interests include robotic vehicle, electric vehicle with in-wheel motor, and vehicle dynamics (independent driving, active steering, and hybrid steering).

Sunghoon Back received his B.S. degree in Aerospace Engineering from Konkuk University in 1996 and his M.S degree in Mechanical Engineering from Konkuk University in 1998. He is working at Hyundai Rotem Company as senior research engineer since July 2003 and currently working toward a Ph.D. Degree in Mechatronics Engineering at Hanyang University. His research interests include advanced vehicle control, unmanned ground vehicle design and multi-sensor-based autonomous driving.

Youngsoo Kim received his B.S. degree in Mechanical Engineering from Soongsil University in 1997 and his M.S degree in Mechanical Engineering from Korea University in 2005. He is currently doing Ph.D. degree in Mechatronics Engineering at Hanyang University. His research interests include multi-axle driving and control, sensor based motion planning.

Soonwoong Hwang received his B.S. degree in Mechanical Engineering from Hanyang University, in 2007 and his M.S. degree in Mechatronics Engineering from Hanyang University in 2009. He is currently working toward a Ph.D. degree in Mechatronics Engineering at Hanyang University. His research interests include intelligent service robot with 7 DOF arms and mobile platform, dynamic performance analysis, and analytical manipulator design.

Jaeho Jang received his B.S. degree in Mechanical Engineering from Hanyang University in 2001; an M.S. degree in Mechatronics Engineering from Hanyang University in 2003; and a Ph.D. degree in Mechanical Engineering from Hanyang University in 2008. He is working at Korea Institute of Industrial Technology since 2008. His research interests include military robot and rehabilitation service robot.

Changsoo Han received his B.S. degree in Mechanical Engineering from Hanyang University, and his M.S. and Ph.D. degrees in Mechanical Engineering from University of Texas at Austin in 1983, 1985, and 1989, respectively. In March 1990, he joined Hanyang University, Ansan, Korea as an assistant professor in the Department of Mechanical Engineering. Currently, he is a Professor with the department of robot engineering, Hanyang University. His research interests include intelligence service robot, high precision robotics and mechatronics, rehabilitation and biomechanics technology using robotics, automation in construction and advanced vehicle control.